Dynamics of Ca^{2+}-Calmodulin–dependent Inhibition of Rod Cyclic Nucleotide-gated Channels Measured by Patch-clamp Fluorometry

Matthew C. Trudeau and William N. Zagotta

Howard Hughes Medical Institute, Department of Physiology and Biophysics, University of Washington Medical School, Seattle, WA 98195

ABSTRACT Cyclic nucleotide-gated (CNG) ion channels mediate cellular responses to sensory stimuli. In vertebrate photoreceptors, CNG channels respond to the light-induced decrease in cGMP by closing an ion-conducting pore that is permeable to cations, including Ca^{2+} ions. Rod CNG channels are directly inhibited by Ca^{2+}-calmodulin (Ca^{2+}/CaM), but the physiological role of this modulation is unknown. Native rod CNG channels comprise three CNGA1 subunits and one CNGB1 subunit. The single CNGB1 subunit confers several key properties on heteromeric channels, including Ca^{2+}/CaM-dependent modulation. The molecular basis for Ca^{2+}/CaM inhibition of rod CNG channels has been proposed to involve the binding of Ca^{2+}/CaM to a site in the NH_2-terminal region of the CNGB1 subunit, which disrupts an interaction between the NH_2-terminal region of CNGB1 and the COOH-terminal region of CNGA1. Here, we test this mechanism for Ca^{2+}/CaM-dependent inhibition of CNGA1/CNGB1 channels by simultaneously monitoring protein interactions with fluorescence spectroscopy and channel function with patch-clamp recording. Our results show that Ca^{2+}/CaM binds directly to CNG channels, and that binding is the rate-limiting step for channel inhibition. Further, we show that the NH_2- and COOH-terminal regions of CNGB1 and CNGA1 subunits, respectively, are in close proximity, and that Ca^{2+}/CaM binding causes a relative rearrangement or separation of these regions. This motion occurs with the same time course as channel inhibition, consistent with the notion that rearrangement of the NH_2- and COOH-terminal regions underlies Ca^{2+}/CaM-dependent inhibition.

KEY WORDS: Ca^{2+}/calmodulin • cyclic nucleotide-gated channels • patch-clamp • fluorescence • FRET

INTRODUCTION

Cyclic nucleotide-gated (CNG) ion channels mediate the transduction of sensory stimuli into electrical signals (Kaupp and Seifert, 2002; Matulef and Zagotta, 2003). In rod and cone photoreceptors, CNG channels close in response to the decrease in concentration of 5′:3′ cyclic guanosine monophosphate (cGMP) that occurs with light absorption (Yau and Baylor, 1989; Burns and Baylor, 2001). In olfactory sensory neurons, CNG channels open in response to the increase in concentration of 5′:3′ cyclic adenosine monophosphate (cAMP) that occurs with odorant binding (Menini, 1999; Zufall and Munger, 2001). CNG channels are also present in other tissues, including the brain, taste receptors, aorta, liver, and kidney, but their roles in these tissues are not as well understood (Richards and Gordon, 2000).

CNG channels are part of a subfamily of ion channels that are regulated by the direct binding of cyclic nucleotides, including the hyperpolarization-activated cyclic nucleotide-modulated (HCN) channels and the ether-a-go-go (eag) K^+ channels (Guy et al., 1991; Robinson and Siegelbaum, 2003). CNG channels are nonselective for cations, but their ion-conducting pore is similar to that of bacterial K^+-selective channels whose three-dimensional structure is known (Doyle et al., 1998; Zhou et al., 2001; Jiang et al., 2002; Flynn and Zagotta, 2003). Like their voltage-activated counterparts, CNG channels have six membrane-spanning domains and internal NH_2- and COOH-terminal regions; however, they are only weakly activated by voltage (Kaupp et al., 1989; Jan and Jan, 1990). Instead, CNG channels are gated (or opened) by the direct binding of cGMP (Fesenko et al., 1985) or cAMP (Nakamura and Gold, 1987) to a COOH-terminal cyclic nucleotide-binding domain (CNBD). The structure of the CNBD and adjoining C-linker region has recently been solved for a related hyperpolarization-activated cyclic nucleotide-modulated (HCN) channel (Zagotta et al., 2003).

Native rod CNG channels comprise CNGA1 subunits and CNGB1 subunits. These channel subunits are 35%

Address correspondence to William N. Zagotta, Dept. of Physiology and Biophysics, Box 357290, University of Washington, Seattle, WA 98195-7290. Fax: (206) 543-0934; email: zagotta@u.washington.edu

M.C. Trudeau's present address is Department of Physiology, University of Maryland School of Medicine, Baltimore, MD 21201.

Abbreviations used in this paper: CaM, calmodulin; cAMP, cyclic adenosine monophosphate; cGMP, cyclic guanosine monophosphate; CNBD, cyclic nucleotide-binding domain; CNG, cyclic nucleotide-gated; eCFP, enhanced cyan fluorescent protein; eYFP, enhanced yellow fluorescent protein; FRET, fluorescence resonance energy transfer; PCF, patch-clamp fluorometry.

J. Gen. Physiol. © The Rockefeller University Press • 0022-1295/2004/09/211/13 $8.00
Volume 124 September 2004 211–223
http://www.jgp.org/cgi/doi/10.1085/jgp.200409101

identical on the amino acid level but functionally quite different. CNGA1 subunits form homomeric CNG channels in heterologous systems with some of the properties of native rod channels (Kaupp et al., 1989). CNGB1 subunits do not form functional homomeric channels; however, coexpression of CNGA1 and CNGB1 subunits results in heteromeric channels that recapitulate many of the biophysical and pharmacological properties of native rod channels (Chen et al., 1993, 1994; Korschen et al., 1995). The CNGB1 subunit confers several new properties on the heteromeric channels, including higher fractional activation by cAMP (a partial agonist of the channels), increased permeability of Ca^{2+} relative to Na^+, native-like single-channel behavior, sensitivity to the blocker L-cis-diltiazem, and sensitivity to inhibition by Ca^{2+}-calmodulin (Ca^{2+}/CaM). Unexpectedly, these properties are produced by only a single CNGB1 subunit, as rod channels contain three CNGA1 subunits and only one CNGB1 subunit (Weitz et al., 2002; Zheng et al., 2002; Zhong et al., 2002; Zimmerman, 2002).

Rod channels, cone channels, and olfactory channels are all inhibited by extrinsic Ca^{2+}/CaM (Hsu and Molday, 1993; Chen and Yau, 1994; Hsu and Molday, 1994; Gordon et al., 1995; Korschen et al., 1995; Bauer, 1996; Hackos and Korenbrot, 1997; Peng et al., 2003). Ca^{2+}/CaM-dependent inhibition of native olfactory channels is a major determinant of olfactory adaptation (Kurahashi and Menini, 1997), and in cone CNG channels, Ca^{2+}/CaM (along with an unknown factor) may form a feedback loop that contributes to light adaptation (Hackos and Korenbrot, 1997; Rebrik and Korenbrot, 1998). In rod CNG channels, the role for Ca^{2+}/CaM-dependent inhibition is unknown. In rod CNG channels, a site was identified in the NH_2-terminal region of the CNGB1 subunit as important for direct Ca^{2+}/CaM binding and functional modification (Grunwald et al., 1998; Weitz et al., 1998; Trudeau and Zagotta, 2002b). Fusion proteins containing this site bound Ca^{2+}/CaM, and deletion of this site rendered channels insensitive to modulation by Ca^{2+}/CaM. In addition, the NH_2-terminal region of CNGB1 subunits and the distal COOH-terminal region of CNGA1 subunits formed a specific interaction in a biochemical interaction assay (Trudeau and Zagotta, 2002a). This interaction required an intact Ca^{2+}/CaM-binding site and was disrupted in the presence of Ca^{2+}/CaM (Trudeau and Zagotta, 2002b). Based on these results, it has been proposed that Ca^{2+}/CaM modulation of rod channels involves Ca^{2+}/CaM binding to a site on the NH_2-terminal region, which disrupts an interaction between the NH_2- and COOH-terminal regions, and causes channel inhibition. A similar but distinct mechanism has been proposed for Ca^{2+}/CaM modulation of homomeric olfactory channels (Varnum and Zagotta, 1997; Trudeau and Zagotta, 2003; Zheng et al., 2003).

In this paper, we have sought to test this mechanism for Ca^{2+}/CaM inhibition using fluorescence methods that offer distinct advantages over previous biochemical and electrophysiological approaches. We find that Ca^{2+}/CaM binding to CNG channels is the rate-limiting step for inhibition. We show that Ca^{2+}/CaM binds in close proximity to the putative Ca^{2+}/CaM-binding site in the NH_2-terminal region of CNGB1. Finally, we show that the NH_2- and COOH-terminal regions of the channel subunits are in close proximity in intact channels, and that these regions undergo a rearrangement with the same time course as Ca^{2+}/CaM-dependent inhibition. These results provide further support for the proposal that Ca^{2+}/CaM inhibition involves a Ca^{2+}/CaM-dependent disruption of an interaction between the NH_2- and COOH-terminal regions.

MATERIALS AND METHODS

Molecular Biology and Oocyte Expression

The CNGA1 clone used here was previously described (Gordon and Zagotta, 1995; Trudeau and Zagotta, 2002a) and was identical to the original clone (Kaupp et al., 1989), except for a K2E change and an eight–amino acid FLAG epitope on the COOH-terminal end. The CNGB1 clone was a gift from R. Molday (University of British Columbia, Vancouver, BC, Canada) (Korschen et al., 1995) and contained an I2V change that did not affect any of the properties studied here. The enhanced cyan fluorescent protein (eCFP) and enhanced yellow fluorescent protein (eYFP) clones were a gift from R.Y. Tsien (University of California, San Diego, CA) (Miyawaki et al., 1997). Fluorescent proteins were genetically attached to CNGA1 and CNGB1 subunits using an overlapping PCR strategy and confirmed with DNA sequencing. In CNGA1-eYFP, eYFP was fused immediately after the FLAG epitope tag at the COOH terminus. In eCFP-CNGB1, eCFP was fused before amino acid 677 of CNGB1 and was immediately upstream of the CaM-binding site (Trudeau and Zagotta, 2002b). eCFPΔCaM-CNGB1 had a deletion mutation of the Ca^{2+}/CaM site (which eliminated an additional 25 amino acids), and the eCFP was fused before amino acid 702 of the CNGB1 subunit. Channel cDNAs were subcloned into the pGEMHE vector (a gift of E. Liman, University of Southern California, Los Angeles, CA) for heterologous expression. RNA was transcribed with the mESSAGE mACHINE kit (Ambion) and injected with a micropipette into *Xenopus* oocytes. Oocytes were prepared as described elsewhere (Gordon et al., 1995) and incubated with shaking for 3–10 d at 16°C.

Patch-clamp Electrophysiology and Fluorescence Imaging

Ionic currents through CNG channels expressed in oocytes were recorded in the excised, inside-out patch-clamp configuration (Hamill et al., 1981) with an Axopatch 200B patch-clamp amplifier (Axon Instruments, Inc.). Data were digitized with an ITC-16 (Instrutech) and recorded and analyzed with the Pulse software package (Instrutech) and Igor software running on a Pentium III computer. The patch pipette (external) solution contained 130 mM NaCl, 0.2 mM EDTA, 3 mM HEPES, pH 7.2 (with 500 μM niflumic acid to block endogenous Cl^- channels). The Ca^{2+}-free bath (internal) solution contained 130 mM NaCl, 0.2 mM EDTA, 3 mM HEPES, pH 7.2, and 50 μM cGMP (Sigma-Aldrich) to acti-

vate CNG channels. In solutions with internal Ca^{2+} ions, (Ca^{2+}-only and Ca^{2+}/CaM), 2 mM NTA replaced EDTA and 50 μM total Ca^{2+} was added to achieve a free Ca^{2+} concentration of 1 μM, as determined with WinMaxC (Bers et al., 1994). CaM (Calbiochem) or CaM conjugated to the fluorescent dye Alexa-488 (CaM-488) (Molecular Probes) was added to Ca^{2+}-containing solutions at a concentration of 250 nM. Internal solutions were applied to the cytoplasmic face of a membrane patch with an RSC-200 solution changer (Molecular Kinetics).

For patch-clamp fluorometry (PCF) experiments, fluorescent signals were recorded by imaging the patch pipette tip with a cooled CCD camera (Princeton Instruments) while the ionic current was simultaneously recorded with a patch-clamp. Fluorescence was observed with a 40× oil-immersion objective (NA 1.3) on a Nikon Diaphot inverted microscope. Fluorophores were excited at the appropriate wavelength using a monochrometer (Cairn) with a xenon lamp light source, and the appropriate excitation filter and dichroic mirror configuration (for eCFP, exciter: 440 ± 10 nm, dichroic: 455 nm; for eYFP or CaM-488, exciter: 470 ± 20 nm, dichroic: 510 nm; Chroma Technology Corp.). Emission spectra were recorded with 10-nm bandpass emission filters (Chroma Technology Corp.) set into a coupled pair of filter wheels (Sutter Instrument Co.). Fluorescence data were acquired and analyzed with the MetaMorph software package (Universal Imaging Corp.).

After a membrane patch was excised, ionic currents were recorded every 10 s with a voltage pulse from −60 to 60 mV (from a holding voltage of 0 mV) in a subsaturating (50 μM) concentration of cGMP. Often there was a characteristic increase in current associated with dephosphorylation after patch excision (Gordon et al., 1992; Molokanova et al., 1997). Experiments were conducted after the current reached a steady level. Ca^{2+}/CaM or Ca^{2+}/CaM-488 was then perfused for a given amount of time while the current was recorded at 10-s intervals. Then CaM (or CaM-488) was removed and replaced with Ca^{2+}-only solution, containing 1 μM Ca^{2+}, and the current was recorded. In the Ca^{2+}-only solution, the previous inhibition by Ca^{2+}/CaM was maintained, and the currents were stable. An emission spectra of nine wavelengths was then determined while the membrane was held at 0 mV. In this way, the ionic current and fluorescent signals were recorded after the same cumulative time in Ca^{2+}/CaM (or Ca^{2+}/CaM-488). This method also minimized solution artifacts, as the spectra were always determined in the presence of the same internal solution (containing 1 μM Ca^{2+}). The time course of channel inhibition by Ca^{2+}/CaM was determined using the cumulative time the patch was exposed to the modifier. To washout Ca^{2+}/CaM (or Ca^{2+}/CaM-488), patches were exposed to Ca^{2+}-free solution (containing 0.2 mM EDTA) for the indicated amount of time, during which time the Ca^{2+}/CaM-dependent inhibition was alleviated. As above, solutions were switched from Ca^{2+}-free solution to Ca^{2+}-only solution for current and fluorescence measurements. The cumulative time refers to the time spent in the Ca^{2+}-free solution.

Over the course of an experiment, the eCFP fluorescence decreased by ~5–10% due to bleaching. The bleaching time course was measured from patches with eCFP-only containing channels subunits and corrected in the time courses of the eCFP fluorescence in Fig. 3 (C and F).

Confocal Microscopy

Emission spectra from whole oocytes expressing fluorescently labeled channel subunits were collected using a confocal microscope (Leica TCS) with laser excitation. The microscope objective was 5× with 0.15 NA. The measurement of spectra was enabled by acousto-optical tunable filters with an emission window of 5 nm. Fluorescence resonance energy transfer (FRET) was measured from the stimulated emission of the acceptor fluorophore (eYFP) with excitation of the donor fluorophore (eCFP). We took a ratiometric approach to solve for the spectral component due to FRET (Selvin, 1995). The experimental spectra with excitation at 458 nm (Fig. 4 A, red) had two components, one at 480 nm due to eCFP and one at 530 nm due to eYFP. The eCFP component of the experimental trace was removed by subtracting a scaled eCFP spectra (Fig. 4 A, cyan) from a control experiment with eCFP-CNGB1/CNGA1 channels. This yielded the extracted spectra (Fig. 4 A, green) due to eYFP emission (F_{458}), which contained two components: the emission due to FRET (F_{458}^{FRET}) and the emission due to the small but finite excitation of eYFP directly by the 458 laser (F_{458}^{direct}). F_{458}^{FRET} was obtained by dividing the extracted spectra F_{458} by the YFP emission spectra with direct excitation at 488 nm (F_{488}; Fig. 4 A, black trace) (Selvin, 1995). This ratio, Ratio A, contained two components.

$$\text{Ratio A} = \frac{F_{458}}{F_{488}} = \frac{F_{458}^{direct}}{F_{488}} + \frac{F_{458}^{FRET}}{F_{488}}$$

The first component (Ratio A_0) was determined with an additional control experiment in which eYFP spectra were measured from CNGA1 channels with only eYFP attached (Fig. 4 B) with excitation at 458 nm (F_{458}; Fig. 4 B, red trace) or 488 nm (F_{488}; Fig. 4 B, black trace), which yielded Ratio A_0.

$$\text{Ratio A}_0 = \frac{F_{458}^{direct}}{F_{488}}$$

The FRET component was calculated by subtracting Ratio A_0 from Ratio A, which yields a value that is proportional to FRET efficiency.

RESULTS

Ca^{2+}/CaM Binding Determines the Rate of CNG Channel Inhibition

To study the mechanism of Ca^{2+}/CaM modulation of rod CNG channels, we used the PCF technique in which fluorescence intensity and ionic current are recorded simultaneously from an inside-out patch of membrane containing fluorescently labeled channels (Zheng and Zagotta, 2000, 2003). PCF provides time-resolved measurements of protein rearrangements in intact functioning channels in the plasma membrane. To directly measure Ca^{2+}/CaM binding we used a CaM molecule that was conjugated to the fluorescent dye Alexa-488 (CaM-488). Fig. 1 A shows that Ca^{2+}/CaM-488 inhibited heteromeric CNGA1/CNGB1 channels expressed in *Xenopus* oocytes. CNG currents were recorded in the inside-out configuration of the patch-clamp technique with voltage steps from −60 to 60 mV in the presence of a subsaturating concentration of cGMP (50 μM) and were leak subtracted (Fig. 1 A). The patch was then exposed to Ca^{2+}/CaM-488 for 3 min followed by a wash in a Ca^{2+}-only solution to remove unbound CaM-488 (but not bound CaM-488). The current was stable in the Ca^{2+}-only solution and was inhibited about twofold (Fig. 1 A, center). After washout of Ca^{2+}/CaM-488 in Ca^{2+}-free solution, the current recovered to its initial value (Fig. 1 A, right).

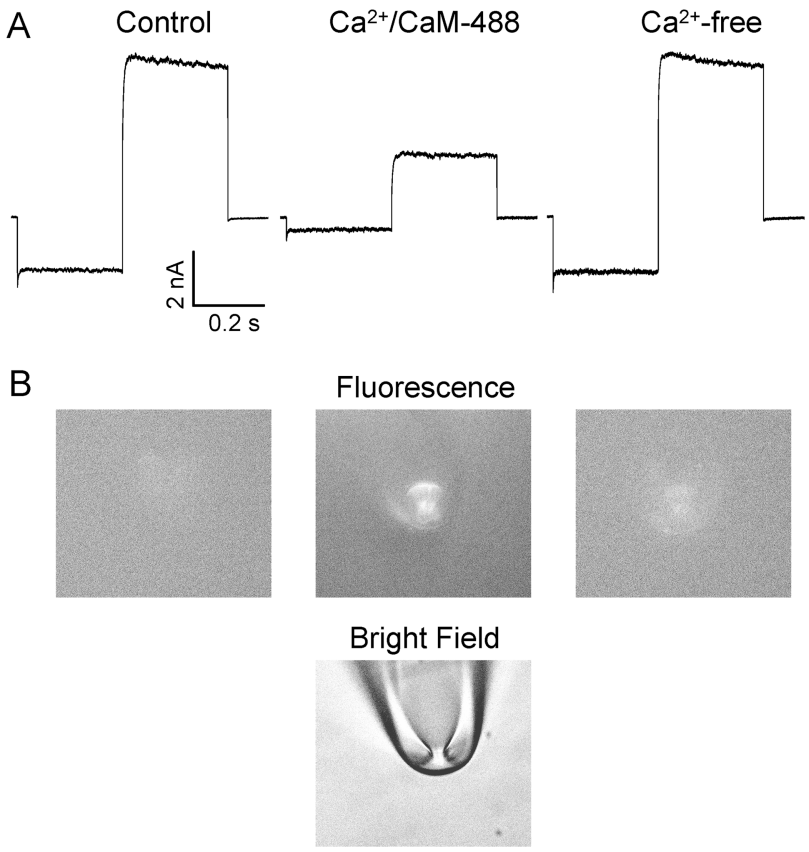

FIGURE 1. Binding of fluorescent Ca^{2+}/CaM to CNG channels. (A) cGMP-activated ionic currents before (left) and after (center) the addition of Ca^{2+}/CaM-488 and after washout (right). All currents were recorded in response to 50 μM cGMP with a voltage pulse from −60 to 60 mV from a holding voltage of 0 mV. (B) Bright field image of patch pipette and fluorescence images before (left) and after (center) addition of Ca^{2+}/CaM-488, and after washout of Ca^{2+}/CaM-488 (right).

To directly measure the binding of Ca^{2+}/CaM-488 we monitored the fluorescence intensity in the membrane patch (Fig. 1 B) while we simultaneously measured the ionic current. The fluorescence intensity at 530 nm was measured in response to excitation at 470 nm. Before addition of Ca^{2+}/CaM-488 there was no detectable fluorescent signal coming from the pipette or patch membrane (Fig. 1 B, left). After addition of Ca^{2+}/CaM-488, followed by washing in a Ca^{2+}-only solution to remove the unbound CaM-488, we observed a large increase in the fluorescence at the pipette tip. No significant fluorescence was detected in patches from uninjected oocytes (not depicted), suggesting that Ca^{2+}/CaM-488 was associating directly with the channels in the membrane patch (Fig. 1 B, center). Upon washout of the Ca^{2+}/CaM-488 in Ca^{2+}-free solution and recovery of the current, the fluorescence of the patch was likewise eliminated (Fig. 1 B, right), indicating that Ca^{2+}/CaM-488 has dissociated from the channels.

To determine if the Ca^{2+}/CaM-488 bound to the membrane was indeed the same Ca^{2+}/CaM-488 that was modulating the channels, we compared the time courses of the changes in ionic current and fluorescence intensity recorded simultaneously (Fig. 2). The time course of the current decrease by Ca^{2+}/CaM-488 is similar to that seen previously for Ca^{2+}/CaM (Grunwald et al., 1998; Weitz et al., 1998; Trudeau and Zagotta, 2002b) (Fig. 2 B). The time course of current inhibition and recovery (Fig. 2 B) was mirrored precisely by the time course of fluorescence intensity increase and decrease (Fig. 2 C). Single exponential fits to these data revealed no significant difference between the time constant of current inhibition ($\tau = 14.7 \pm 2.0$ s, $n = 3$) and the time constant for fluorescence increase ($\tau = 18.5 \pm 2.3$ s, $n = 3$). Similarly there was no significant difference between the time constant of current recovery ($\tau = 68 \pm 19$ s, $n = 3$) and the time constant for fluorescence decrease ($\tau = 51 \pm 20$ s, $n = 3$). This similarity between the ionic current and fluorescence intensity time courses suggests that the Ca^{2+}/CaM-488 bound to the membrane was indeed the same Ca^{2+}/CaM-488 that was modulating the channels. The single exponential time course of the fluorescence change is consistent with a single Ca^{2+}/CaM-488 binding to the intact channel, as expected from the 3:1 CNGA1:CNGB1 stoichiometry of the channel. Finally, the similarity between the current and fluorescence time courses indicates that the binding of Ca^{2+}/CaM is the rate-limiting step for channel inhibition.

Ca^{2+}/CaM Binds in Close Proximity to a Putative Ca^{2+}/CaM-binding Site in the CNGB1 Subunit

The previous experiment suggests that Ca^{2+}/CaM binds to a constituent of the membrane patch and is associ-

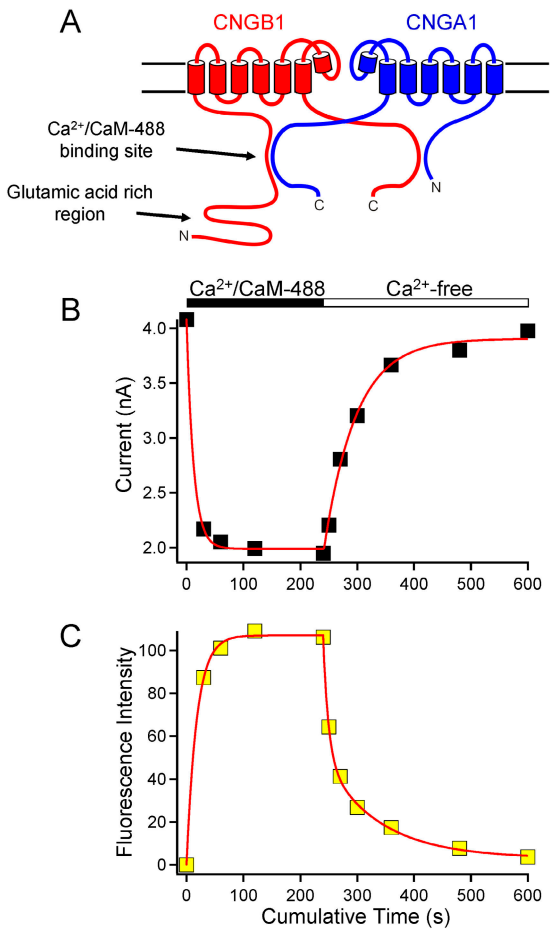

FIGURE 2. Ionic current and fluorescence during Ca^{2+}/CaM-dependent modulation. (A) Cartoon image depicting two (of four) subunits in rod CNGA1/CNGB1 channels. (B) Time course of ionic current and (C) fluorescence intensity with the addition (black bar) and washout (open bar) of Ca^{2+}/CaM-488. Red lines show single-exponential fits to the data points.

ated with inhibition of CNG channels. Here, using FRET, we show that Ca^{2+}/CaM binds directly to intact CNG channels. FRET is the transfer of energy from an excited donor fluorophore to an acceptor fluorophore when the molecules are within a permissive distance (<80 Å) (see Lakowicz, 1999). Ca^{2+}/CaM-488 has spectral properties similar to eYFP, and thus can be used as the acceptor in a FRET pair, with eCFP as the donor, to monitor proximity (Heim and Tsien, 1996). We genetically attached eCFP to the NH_2-terminal region of the CNGB1 channel subunit at a site immediately adjacent to the putative Ca^{2+}/CaM-binding site (eCFP-CNGB1) (Fig. 3 A). We then monitored FRET between eCFP on CNGB1 and Ca^{2+}/CaM-488 by measuring the quenching of eCFP fluorescence (which was excited at 440 nm) by the nearby Alexa-488 dye.

Using PCF, we simultaneously measured the current and eCFP fluorescence intensity during the application and removal of Ca^{2+}/CaM-488 to inside-out patches containing CNGA1/eCFP-CNGB1 channels. As before, the indicated solution was applied for various amounts of time, followed by a wash in Ca^{2+}-only solution, at which point the current and fluorescence were measured. We found that the eCFP (donor) emission decreased (quenched) in the presence of Ca^{2+}/CaM-488 (acceptor) (Fig. 3 C). Furthermore, the time course of eCFP quenching (τ = 24.6 ± 6.8 s, n = 4) precisely matched the time course of ionic current decay (τ = 23.1 ± 9.2 s, n = 4) (Fig. 3, B and C). During the washout of CaM-488 in Ca^{2+}-free solution, current recovery again had a time course (τ = 61 ± 6 s, n = 4) similar to the time course of recovery of eCFP fluorescence (dequenching) (τ = 129 ± 20 s, n = 4). We note that while similar, the eCFP recovery was about twofold slower than the current recovery. The reason for this small difference is not clear, given the matching recovery time courses of current and fluorescence in Figs. 2 and 6. The occurrence of FRET in these experiments (Fig. 3 C) indicates that Ca^{2+}/CaM binds within close proximity (<80 Å) to the Ca^{2+}/CaM-binding site in the NH_2-terminal region of CNGB1, suggesting a direct association between Ca^{2+}/CaM and CNGB1 subunits in intact channels.

As a control experiment, we deleted the putative Ca^{2+}/CaM-binding region from the NH_2-terminal region of CNGB1 (eCFP-CNGB1ΔCaM) and coexpressed these subunits with CNGA1 subunits (Fig. 3 D). The resultant heteromeric channels were insensitive to Ca^{2+}/CaM (Fig. 3 E). Likewise, the eCFP fluorophore was not quenched when Ca^{2+}/CaM-488 was introduced (Fig. 3 F). These results confirm that this region is necessary for binding of Ca^{2+}/CaM to CNGB1 and inhibition of CNGA1/CNGB1 channels by Ca^{2+}/CaM.

NH_2- and COOH-terminal Regions Are in Close Proximity

What are the molecular regions of CNG channels that underlie channel inhibition by Ca^{2+}/CaM? Previously, using polypeptide fragments from the channels, we showed that a physical interaction existed between the NH_2- and COOH-terminal regions of CNGB1 and CNGA1 subunits, respectively (Trudeau and Zagotta, 2002a,b). We sought to study this interaction in intact CNG channels with FRET spectroscopy. Fluorescent proteins were fused next to the cytoplasmic regions of the CNG channel subunits that were previously shown to interact. Specifically, eCFP was attached proximal to the NH_2-terminal Ca^{2+}/CaM-binding region of CNGB1 and eYFP was attached to the distal COOH-terminal region of CNGA1 (Fig. 4).

First, we measured FRET from these CNGA1-eYFP/eCFP-CNGB1 channels in whole oocytes by measuring the stimulated emission of eYFP due to excitation of a nearby eCFP. The emission spectra were measured just from the surface membrane using a confocal micro-

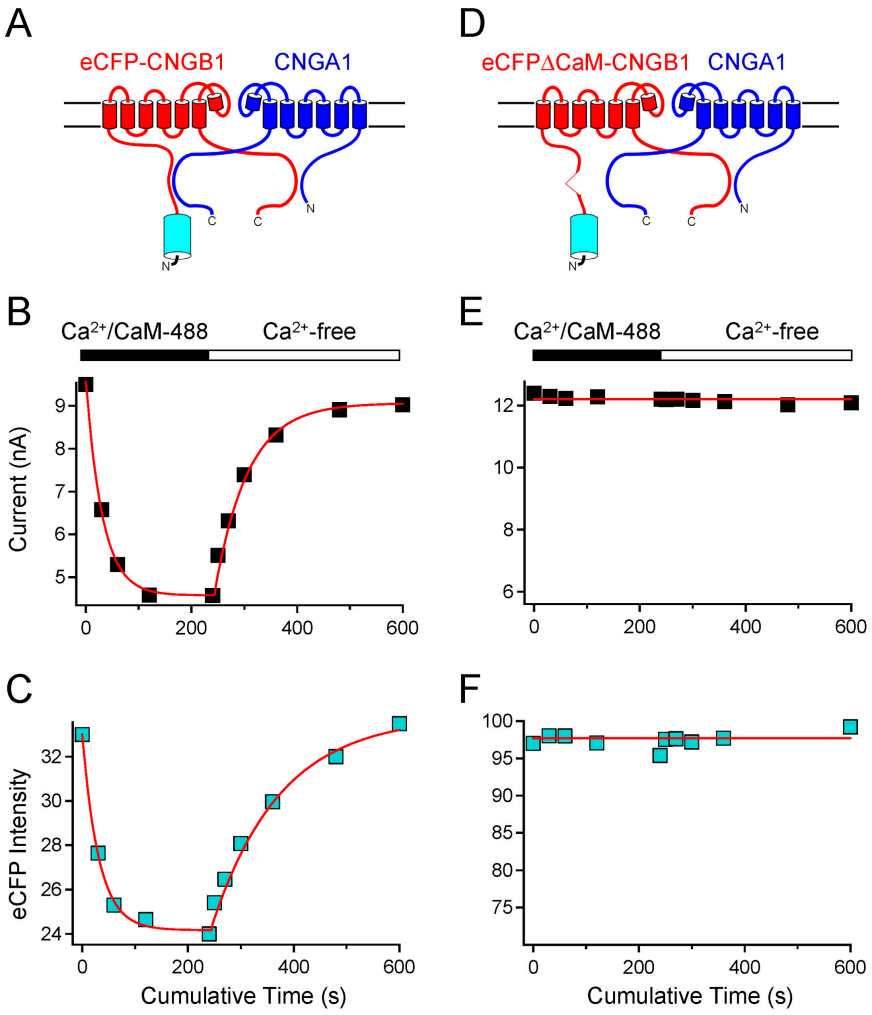

FIGURE 3. FRET between Ca^{2+}/CaM-488 and an eCFP on the CNGB1 subunit. (A) Cartoon depicting eCFP-CNGB1 in which an eCFP molecule is genetically attached to the NH_2-terminal region of CNGB1, adjacent to the Ca^{2+}/CaM-binding site. (B) Ionic currents and (C) eCFP fluorescence intensities measured at 480 nm with the addition (black bar) and washout (open bar) of Ca^{2+}/CaM-488. A decrease in eCFP intensity indicates FRET and close proximity with Ca^{2+}/CaM-488. (D) Depiction of CNGA1/eCFPΔCaM-CNGB1 channels in which the NH_2-terminal CaM-binding site of CNGB1 was deleted. (E) Ionic currents and (F) eCFP intensities in channels lacking a Ca^{2+}/CaM-binding site.

scope. Excitation of eCFP at 458 nm produced a complex emission spectrum with a small peak at ~480 nm, corresponding to eCFP, and a larger peak at ~530 nm, corresponding to eYFP (Fig. 4 A, red trace). To determine the spectral component due to just eYFP, we first subtracted off a scaled spectra from an oocyte expressing only eCFP-fused channel subunits (Fig. 4 A, dashed cyan trace). This yielded just the eYFP component of the spectra (F_{458}; Fig. 4 A, green trace). To determine the eYFP component due to FRET, we took a ratiometric approach (MATERIALS AND METHODS; Selvin, 1995) in which F_{458} is normalized by the eYFP emission after direct excitation of eYFP at 488 nm (F_{488}; Fig. 4 A, black trace). The F_{458}/F_{488} ratio (Ratio A) contained a FRET component as well as a component due to direct excitation of eYFP by the 458-nm laser. The direct component was determined by subtracting the F_{458}/F_{488} ratio (Ratio A_0) in a control experiment in which CNG channels contained only eYFP (Fig. 4 B). The quantity Ratio A − Ratio A_0 is directly proportional to FRET.

For CNGA1-eYFP/eCFP-CNGB1 channels, the Ratio A − Ratio A_0 was significantly greater than zero, indicating FRET (Fig. 5). This suggests that the NH_2- and COOH-terminal regions of CNGB1 and CNGA1, respectively, are within close proximity in intact, heteromeric CNG channels. We have also previously shown that the Ca^{2+}/CaM-binding site is necessary for the biochemical interaction with COOH-terminal fragments of CNGA1 subunits (Trudeau and Zagotta, 2002b). Deletion of the Ca^{2+}/CaM region from CNGB1 (eCFPΔCaM-CNGB1) caused a significant ($P < 0.05$, Student's t test) reduction in FRET of 29% (Fig. 5), consistent with the NH_2- and COOH-terminal regions being further apart or reoriented in the absence of the Ca^{2+}/CaM-binding domain. While reduced, some FRET still remained in channels with the eCFPΔCaM-CNGB1 deletion, presumably because the fluorophores were still within a permissive distance for FRET. It is possible that deletion of the CaM-binding site in eCFPΔCaM-CNGB1 simply shortened the NH_2-terminal region and increased the distance between the CNGB1 NH_2-terminal region and the CNGA1 COOH-terminal region (and the attached fluorophores), reducing FRET. However, our results with Ca^{2+}/CaM

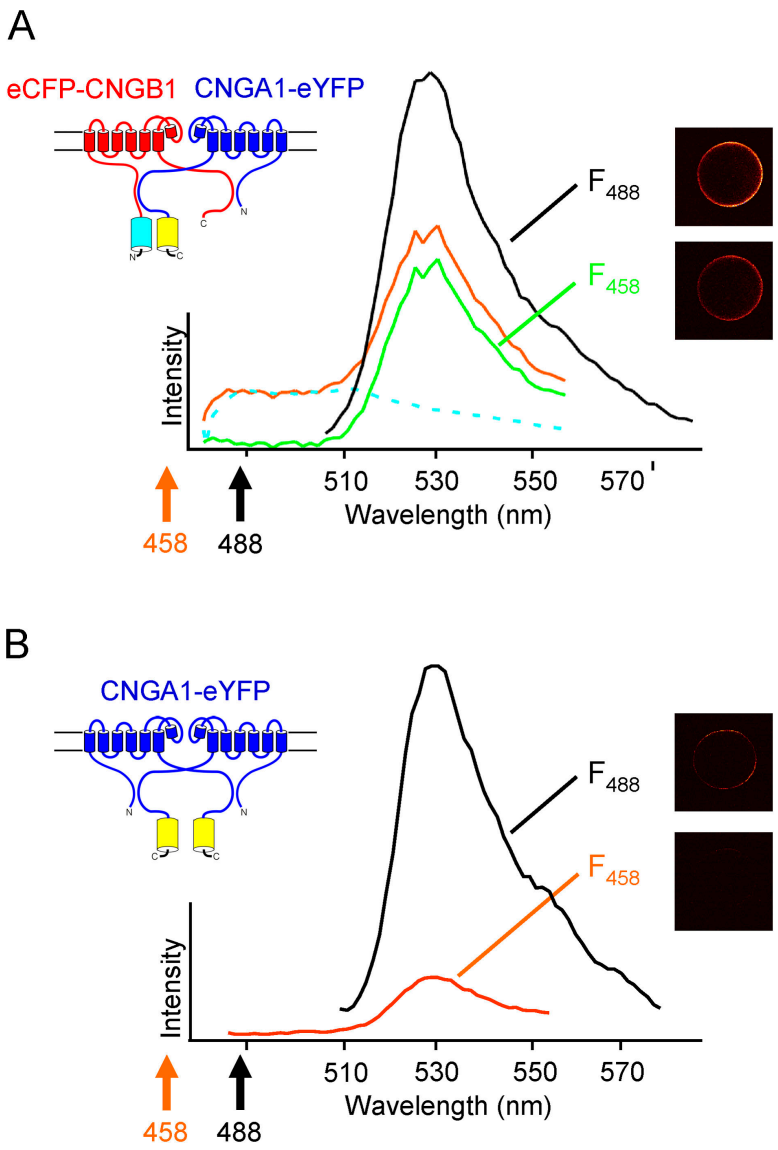

FIGURE 4. Proximity of the NH_2-terminal region of CNGB1 and the COOH-terminal region of CNGA1. (A) Spectral method for determining FRET and Ratio A. Emission spectra from whole oocytes were taken from CNGA1-eYFP/eCFP-CNGB1 channels with eCFP attached to the NH_2-terminal region of CNGB1 and eYFP attached to the COOH-terminal region of CNGA1 (as in the cartoon) with excitation by a 458-nm laser (red line). The eCFP-only spectra (dotted, cyan line) was determined in a separate experiment with channels that contained only eCFP. The extracted F^{458} spectra (green line) is the red minus the cyan trace. F^{488} (black line) is the eYFP emission with excitation by a 488-nm laser. Ratio A was calculated as the F^{458} spectra normalized by the F^{488} spectra. (B) Determination of Ratio A_0. In a control experiment with CNG channels containing only eYFP (cartoon) we determined the emission spectra from eYFP with excitation at 458 nm, F^{458} (red trace), and the emission spectra with excitation at 488 nm, F^{488} (black trace). Ratio A_0 was calculated as the F^{458} spectra normalized by the F^{488} spectra in channels containing only eYFP.

(shown below) are more consistent with a mechanism where deletion of the Ca^{2+}/CaM-binding site disrupted an interaction between the CNGB1 NH_2-terminal region and the CNGA1 COOH-terminal region.

Molecular Rearrangements Between NH_2- and COOH-terminal Regions Underlie Ca^{2+}/CaM-dependent Inhibition

The NH_2-terminal region of CNGB1 and the COOH-terminal region of CNGA1 are in close proximity, and we wished to determine if these regions undergo molecular rearrangements during modulation by Ca^{2+}/CaM. To test this, we expressed CNGA1-eYFP/eCFP-CNGB1 channels (Fig. 6 A) and then introduced Ca^{2+}/CaM to the internal face of membrane patches while simultaneously measuring the ionic current and fluorescence spectra using PCF. In the presence of Ca^{2+}/CaM, the channels were inhibited to the same extent and with the same time course (Fig. 6 B) as channels that do not contain fluorescent proteins (Fig. 2 B), indicating that the fluorophores did not alter the Ca^{2+}/CaM-dependent inhibition of the channels.

We measured emission spectra from these fluorescent channels with 440-nm excitation during the application and washout of Ca^{2+}/CaM and plotted the ratio of the eYFP emission (F^{530}) to the eCFP emission (F^{480}). The F^{530}/F^{480} ratio is related to FRET efficiency, increasing as FRET increases and decreasing as FRET decreases. The initial F^{530}/F^{480} ratio (1.8 ± 0.15, $n = 4$) decreased, with cumulative time in Ca^{2+}/CaM, to a lower F^{530}/F^{480} ratio (1.54 ± 0.09, $n = 4$), indicating a decrease in FRET (Fig. 6 C). This suggests that the NH_2- and COOH-terminal regions rearrange and perhaps separate in the presence of Ca^{2+}/CaM. The time course of the current decay ($\tau = 22.6 \pm 7.1$ s, $n = 5$) and recovery ($\tau = 35.2 \pm 10.3$ s, $n = 5$) was also closely

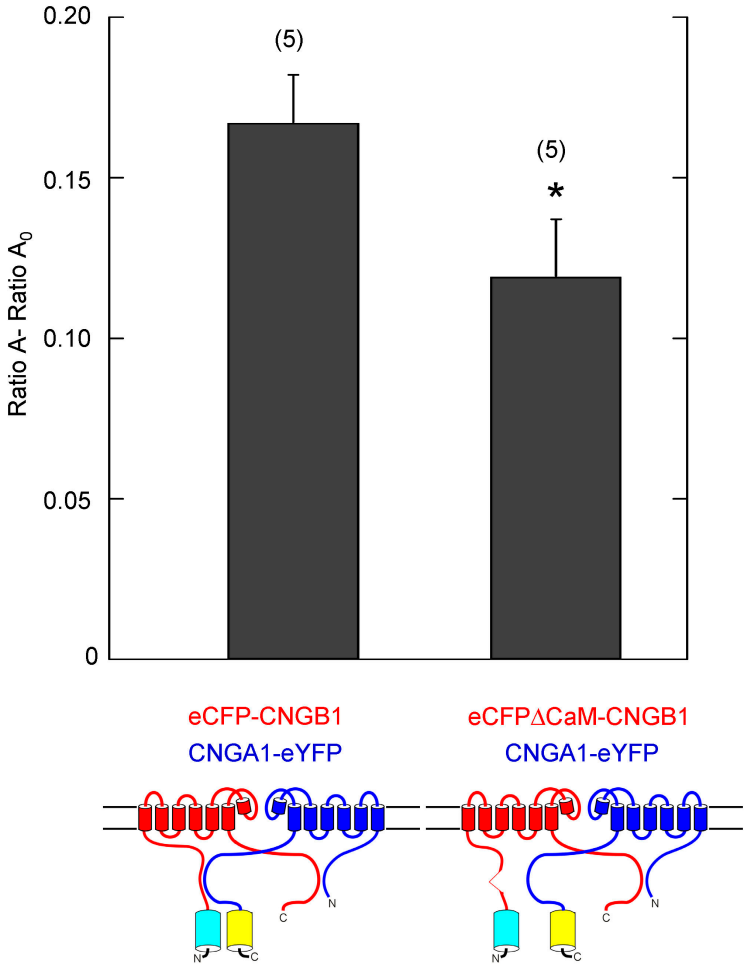

FIGURE 5. Reduction of FRET by deletion of a Ca^{2+}/CaM-binding site. Bar graph of Ratio A–Ratio A_0, which is proportional to FRET, for the indicated eCFP- and eYFP-containing CNG channels. A 29% reduction in FRET was found for channels lacking the Ca^{2+}/CaM-binding site in the NH_2-terminal region of CNGB1.

matched by the time course of F^{530}/F^{480} decrease (τ = 40.7 ± 12.1 s, n = 5) and increase (τ = 32.8 ± 6.1 s, n = 5). The similar time courses suggest that a molecular rearrangement between the NH_2- and COOH-terminal regions is involved in the Ca^{2+}/CaM inhibition of CNGA1/CNGB1 channels.

In a control experiment in which the Ca^{2+}/CaM-binding region was deleted from the CNGB1 subunit (Fig. 6 D), we did not detect inhibition of channels by Ca^{2+}/CaM (Fig. 6 E). We also did not detect a change in FRET in these channels (Fig. 6 F), as the initial F^{530}/F^{480} ratio (1.39 ± 0.08, n = 3) was the same as the F^{530}/F^{480} ratio after a 4-min cumulative exposure to Ca^{2+}/CaM (1.36 ± 0.05, n = 3). This result is consistent with the notion that the Ca^{2+}/CaM-binding region is necessary for the rearrangement between the NH_2- and COOH-terminal regions of CNGB1 and CNGA1. The F^{530}/F^{480} ratio in intact channels in the presence of Ca^{2+}/CaM (1.54 ± 0.09, n = 4) (Fig. 6 C) was similar to that in channels with the Ca^{2+}/CaM site deleted (1.39 ± 0.08, n = 3) (Fig. 6 F), indicating that Ca^{2+}/CaM caused a rearrangement in the channels that was equivalent to removal of the Ca^{2+}/CaM-binding site.

DISCUSSION

Using fluorescence spectroscopy, we have made a number of novel findings regarding inhibition of rod CNG channels by Ca^{2+}/CaM. A major advantage in using fluorescence microscopy over previous biochemical investigations is that we could examine intact channels that are membrane embedded and therefore in an environment approximating their native one. Here we have shown that (a) Ca^{2+}/CaM binding is the rate-limiting step for channel inhibition, (b) Ca^{2+}/CaM binds in close proximity to the NH_2-terminal Ca^{2+}/CaM-binding site of the CNGB1 subunit in intact, functioning heteromeric channels, (c) the NH_2-terminal region of the CNGB1 subunit is in close proximity to the COOH-terminal region of CNGA1 subunits, and (d) the NH_2-terminal region of the CNGB1 subunit and the distal COOH-terminal region of the CNGA1 subunits undergo a relative rearrangement or separation as a consequence of Ca^{2+}/CaM binding, and that this movement is coupled to channel inhibition by Ca^{2+}/CaM.

The proposed mechanism for Ca^{2+}/CaM-dependent inhibition of rod CNG channels is presented in Fig. 7. It postulates that rod CNG channels have an inter-

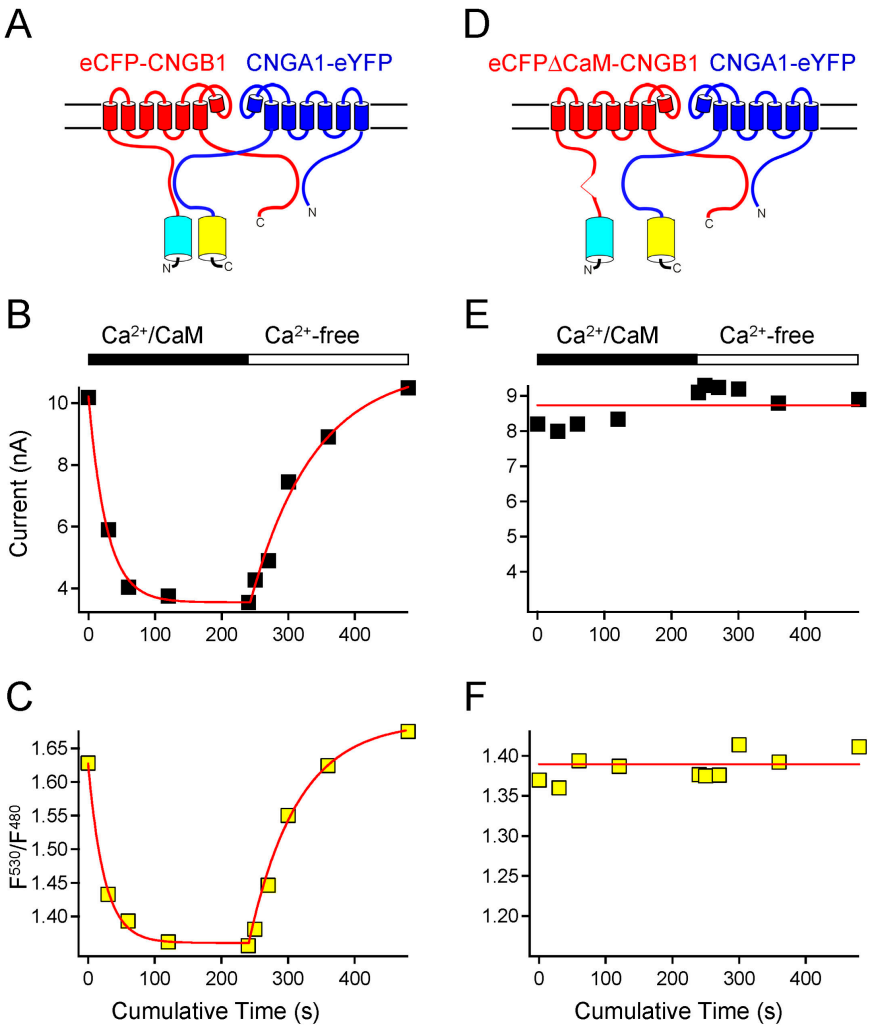

FIGURE 6. Ca^{2+}/CaM-dependent rearrangements in fluorescent channels. (A) Depiction of CNGA1-eYFP/eCFP-CNGB1 channel. (B) Time course of change in ionic current and (C) fluorescence ratio (F^{530}/F^{480}) with the addition (black bar) and washout (open bar) of Ca^{2+}/CaM. (D) Depiction of CNGA1-eYFP/eCFPΔCaM-CNGB1 channels with a deletion of the NH_2-terminal Ca^{2+}/CaM-binding site in CNGB1. The time course of the (E) ionic current and (F) fluorescence ratio in channels lacking the NH_2-terminal binding site.

subunit interaction between the NH_2-terminal region (including a Ca^{2+}/CaM-binding site) of CNGB1 subunits and the distal COOH-terminal region of CNGA1 subunits (Fig. 7 A). Ca^{2+}/CaM binds directly to the CNGB1 subunit, and this is the rate-limiting step in channel inhibition. Upon binding, Ca^{2+}/CaM causes a rearrangement or separation of the NH_2- and COOH-terminal regions of CNGB1 and CNGA1 subunits, respectively (Fig. 7 B). We propose that this rearrangement underlies channel inhibition. Since only a single CNGB1 subunit is present in the CNG channel tetramer, a single Ca^{2+}/CaM molecule appears to be sufficient for channel inhibition.

FRET is an excellent technique for the measurement of the dynamics of rearrangements within a protein or between proteins. What, if anything, can we say about absolute distances? FRET efficiency, which is steeply dependent on distance, is also dependent on κ^2, a value that depends on the relative orientation of fluorophores (Lakowicz, 1999). If the fluorophores are highly mobile, κ^2 can be estimated based on the average of the possible orientations of the fluorophores, and the resulting distance calculated with reasonable accuracy (dos Remedios and Moens, 1995). However, restricted mobility of the fluorophores renders absolute distance calculations meaningless. Absolute efficiency also requires stoichiometric numbers of fluorophores (Lakowicz, 1999). In our experiments, we either have one eCFP to three eYFP's or, for CaM-488, two Alexa-488 fluorophores to one eCFP (the molar ratio of Alexa-488 to CaM is usually 2:1). Thus, we cannot make estimates regarding absolute distances from our results.

Like rod channels, olfactory CNG channels are also inhibited by Ca^{2+}/CaM (Chen and Yau, 1994; Liu et al., 1994; Bradley et al., 2001; Munger et al., 2001). Ca^{2+}/CaM-dependent inhibition of olfactory channels decreases the apparent affinity for cAMP by ~10-fold, which is much larger than the decrease in apparent cGMP affinity in rod channels, which is about twofold (Hsu and Molday, 1993; Chen and Yau, 1994; Liu et al., 1994; Gordon et al., 1995; Grunwald et al., 1998; Weitz et al., 1998). The mechanism of inhibition in homomeric olfactory channels involves the disruption of an interaction between the NH_2-terminal region and

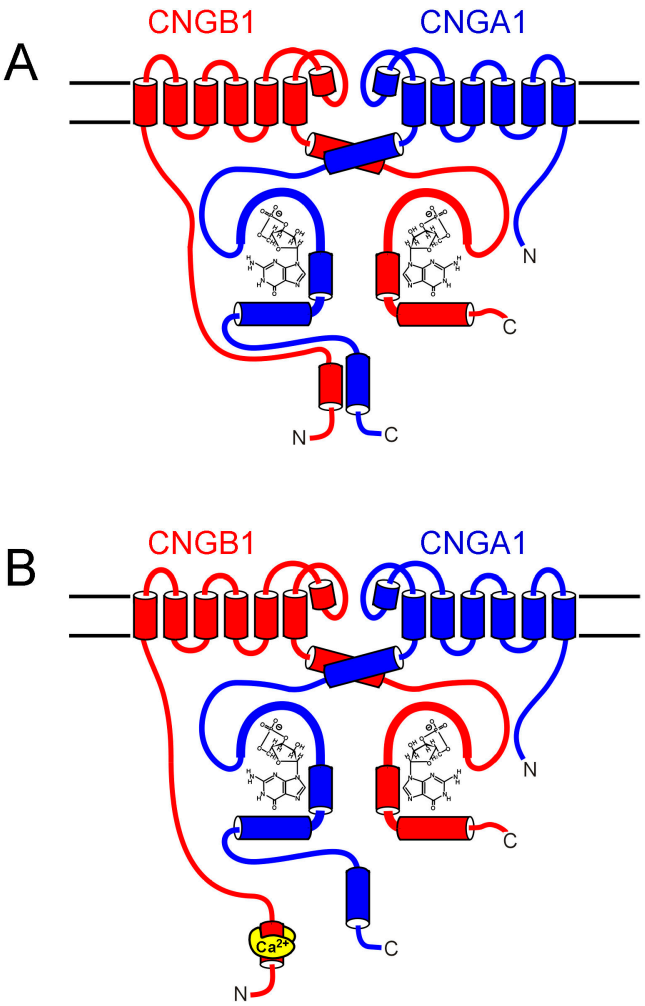

FIGURE 7. Molecular mechanism of Ca^{2+}/CaM-dependent inhibition of CNGA1/CNGB1 channels. (A) Depiction of an intersubunit interaction between the NH_2-terminal region of CNGB1 subunits and the distal COOH-terminal region of CNGA1 subunits. (B) Ca^{2+}/CaM binding to the NH_2-terminal Ca^{2+}/CaM-binding site in CNGB1 results in a rearrangement or separation between the NH_2-terminal region of CNGB1 and the COOH-terminal region of CNGA1.

COOH-terminal region of CNGA2 subunits (Varnum and Zagotta, 1997; Zheng et al., 2003). This interaction occurs between subunits, rather than within a subunit, and the NH_2- and COOH-terminal regions undergo a relative rearrangement with respect to one another (Zheng and Zagotta, 2003). In a broad sense, the mechanisms of inhibition in olfactory and rod channels are similar, but in detail they are quite different. The Ca^{2+}/CaM-binding site in CNGA2 subunits is a 1-8-14 type of binding motif, whereas the binding site in the NH_2-terminal region of CNGB1 subunits is unconventional, but has some similarities to IQ motifs. The NH_2-terminal region of CNGA2 channels has an autoexcitatory effect on channel opening, and deletion of the Ca^{2+}/CaM-binding site in this region reduces the apparent affinity of the channels for cAMP by 10-fold (Liu et al., 1994; Varnum and Zagotta, 1997). In contrast, the NH_2-terminal Ca^{2+}/CaM-binding site in CNGB1 subunits does not appear to have an excitatory effect on channel opening, as deletion of this region does not change the apparent affinity of channels for cyclic nucleotides (Trudeau and Zagotta, 2002b). In both rod and homomeric olfactory channels there is an interaction between the NH_2-terminal region of the channels and the COOH-terminal region, although the specific regions that interact are not related. The autoexcitatory effect of the NH_2-terminal region of CNGA2 subunits is mediated through an interaction with the COOH-terminal CNBD and the C-linker region of olfactory subunits (Varnum and Zagotta, 1997). In rod channels, the NH_2-terminal region of CNGB1 subunits interacts with a region distal to the CNBD in CNGA1 subunits (Trudeau and Zagotta, 2002a). In both rod and olfactory channels, Ca^{2+}/CaM disrupted NH_2- and COOH-terminal interactions, leading to inhibition. In homomeric olfactory channels, Ca^{2+}/CaM disrupted the autoexcitatory effect of the NH_2-terminal region, which can completely account for the change in the apparent affinity for cAMP. In contrast, in rod channels, Ca^{2+}/CaM disrupted an interaction that is not autoexcitatory, but rather, Ca^{2+}/CaM may directly inhibit the channels.

The native olfactory CNG channels are made up of three different CNG channel subunits, CNGA2, CNGA4, and CNGB1b, an alternatively spliced form of CNGB1 (Dhallan et al., 1990; Bradley et al., 1994; Liman and Buck, 1994; Sautter et al., 1998; Bonigk et al., 1999) with a stoichiometry of 2:1:1 (Zheng and Zagotta, 2004). All three subunit types are necessary to reconstitute the fast Ca^{2+}/CaM-dependent inhibition seen in native olfactory channels (Sautter et al., 1998; Bonigk et al., 1999; Bradley et al., 2001; Munger et al., 2001). Recently it has been shown that the rapid Ca^{2+}/CaM modulation of these heteromeric olfactory channels involves the Ca^{2+}/CaM-binding site in the NH_2-terminal region of CNGB1b, identical to the site on CNGB1, and perhaps another site on the CNGA4 subunit (Bradley et al., 2004). Therefore the mechanism for the modulation in heteromeric olfactory channels may have many similarities to the mechanism described here.

Cone channels are also inhibited by Ca^{2+}/CaM. Like rod channels, Ca^{2+}/CaM reduces the apparent affinity of cone channels for cGMP by about twofold (Hackos and Korenbrot, 1997; Rebrik and Korenbrot, 1998; Peng et al., 2003). CNGA3 and CNGB3 subunits are required to recapitulate the properties of native cone channels (Weyand et al., 1994; Gerstner et al., 2000), and both CNGA3 and CNGB3 subunits are required for functional modification by Ca^{2+}/CaM (Peng et al., 2003). The mechanism of Ca^{2+}/CaM-dependent inhi-

bition in cone channels involves two Ca^{2+}/CaM-binding sites in CNGB3 subunits, one on the NH_2-terminal region and one on the COOH-terminal region. Deletion of both sites was necessary to remove Ca^{2+}/CaM inhibition (Peng et al., 2003). Thus, the mechanism of cone channel inhibition appears quite distinct from that in rod or olfactory channels.

A role for Ca^{2+}/CaM-dependent modulation of CNG channels in photoreceptor function is not firmly established. Ca^{2+} ions, CaM, and CNG channels have been theorized to form a feedback system that may play a role in range extension and adaptation in photoreceptors (Hsu and Molday, 1993). This view, however, has been challenged on various grounds. The effect of Ca^{2+}/CaM on CNG channels is relatively modest, compared with the large range over which adaptation occurs (Koutalos et al., 1995; Nakatani et al., 1995). The Ca^{2+} levels in native rods falls from 500 nM in the dark to 50 nM in bright light (Gray-Keller and Detwiler, 1994; Sagoo and Lagnado, 1996), whereas the half maximal concentration for Ca^{2+}/CaM association with channels is 50 nM Ca^{2+} (Hsu and Molday, 1993). This means that at low Ca^{2+} levels in rods, Ca^{2+}/CaM may only partially dissociate from CNG channels, resulting in a smaller dynamic range of inhibition in native channels than that seen in heterologous systems. Nevertheless, a physiological role for Ca^{2+}/CaM-dependent inhibition of rod channels cannot be ruled out. In rods, an unidentified endogenous factor, which appears distinct from CaM, inhibits CNG channels in a Ca^{2+}-dependent manner (Gordon et al., 1995). In native cone channels there is also evidence for an inhibitory cytoplasmic factor that dissociates from channels in zero Ca^{2+} (Rebrik and Korenbrot, 1998). These unidentified factors could be the physiological inhibitors or regulators of native rod and cone CNG channels. In native olfactory channels, however, the role of Ca^{2+}/CaM inhibition is much more clear, where inhibition accounts for perhaps all the negative feedback and adaptation to odorants (Kurahashi and Menini, 1997).

We thank the following people for the generous gift of DNA constructs: R. Molday for CNGB1, R.Y. Tsien for eCFP and eYFP, and E. Liman for pGEMHE. We are grateful to Heidi Utsugi, Kevin Black, Gay Sheridan, and Shellee Cunnington for technical assistance, Greg Martin and Paulette Brunner of the Keck Imaging Center for help with confocal microscopy, and to members of the Zagotta lab for insightful discussions. We thank Michael Varnum and Ariela Gordon-Shagg for comments on an earlier version of the manuscript.

This work was supported by the Howard Hughes Medical Institute and a grant from the National Eye Institute (EY10329) to W.N. Zagotta.

David C. Gadsby served as editor.

Submitted: 17 May 2004
Accepted: 14 July 2004

REFERENCES

Bauer, P.J. 1996. Cyclic GMP-gated channels of bovine rod photoreceptors: affinity, density and stoichiometry of Ca^{2+}-calmodulin binding sites. *J. Physiol.* 494:675–685.

Bers, D., C. Patton, and R. Nuccitelli. 1994. Methods in cell biology. *In* Methods in Cell Biology. Vol. 40. Academic Press, San Diego. 3–29.

Bonigk, W., J. Bradley, F. Muller, F. Sesti, I. Boekhoff, G.V. Ronnett, U.B. Kaupp, and S. Frings. 1999. The native rat olfactory cyclic nucleotide-gated channel is composed of three distinct subunits. *J. Neurosci.* 19:5332–5347.

Bradley, J., J. Li, N. Davidson, H.A. Lester, and K. Zinn. 1994. Heteromeric olfactory cyclic nucleotide-gated channels: a subunit that confers increased sensitivity to cAMP. *Proc. Natl. Acad. Sci. USA.* 91:8890–8894.

Bradley, J., D. Reuter, and S. Frings. 2001. Facilitation of calmodulin-mediated odor adaptation by cAMP-gated channel subunits. *Science.* 294:2176–2178.

Bradley, J., W. Bonigk, K.W. Yau, and S. Frings. 2004. Calmodulin permanently associates with rat olfactory CNG channels under native conditions. *Nat. Neurosci.* 7:705–710.

Burns, M.E., and D.A. Baylor. 2001. Activation, deactivation, and adaptation in vertebrate photoreceptor cells. *Annu. Rev. Neurosci.* 24:779–805.

Chen, T.Y., and K.W. Yau. 1994. Direct modulation by Ca^{2+}-calmodulin of cyclic nucleotide-activated channel of rat olfactory receptor neurons. *Nature.* 368:545–548.

Chen, T.Y., Y.W. Peng, R.S. Dhallan, B. Ahamed, R.R. Reed, and K.W. Yau. 1993. A new subunit of the cyclic nucleotide-gated cation channel in retinal rods. *Nature.* 362:764–767.

Chen, T.Y., M. Illing, L.L. Molday, Y.T. Hsu, K.W. Yau, and R.S. Molday. 1994. Subunit 2 (or beta) of retinal rod cGMP-gated cation channel is a component of the 240-kDa channel-associated protein and mediates Ca^{2+}-calmodulin modulation. *Proc. Natl. Acad. Sci. USA.* 91:11757–11761.

Dhallan, R.S., K.W. Yau, K.A. Schrader, and R.R. Reed. 1990. Primary structure and functional expression of a cyclic nucleotide-activated channel from olfactory neurons. *Nature.* 347:184–187.

dos Remedios, C.G., and P.D. Moens. 1995. Fluorescence resonance energy transfer spectroscopy is a reliable "ruler" for measuring structural changes in proteins. Dispelling the problem of the unknown orientation factor. *J. Struct. Biol.* 115:175–185.

Doyle, D.A., J. Morais Cabral, R.A. Pfuetzner, A. Kuo, J.M. Gulbis, S.L. Cohen, B.T. Chait, and R. MacKinnon. 1998. The structure of the potassium channel: molecular basis of K^+ conduction and selectivity. *Science.* 280:69–77.

Fesenko, E.E., S.S. Kolesnikov, and A.L. Lyubarsky. 1985. Induction by cyclic GMP of cationic conductance in plasma membrane of retinal rod outer segment. *Nature.* 313:310–313.

Flynn, G.E., and W.N. Zagotta. 2003. A cysteine scan of the inner vestibule of cyclic nucleotide-gated channels reveals architecture and rearrangement of the pore. *J. Gen. Physiol.* 121:563–582.

Gerstner, A., X. Zong, F. Hofmann, and M. Biel. 2000. Molecular cloning and functional characterization of a new modulatory cyclic nucleotide-gated channel subunit from mouse retina. *J. Neurosci.* 20:1324–1332.

Gordon, S.E., and W.N. Zagotta. 1995. A histidine residue associated with the gate of the cyclic nucleotide-activated channels in rod photoreceptors. *Neuron.* 14:177–183.

Gordon, S.E., D.L. Brautigan, and A.L. Zimmerman. 1992. Protein phosphatases modulate the apparent agonist affinity of the light-regulated ion channel in retinal rods. *Neuron.* 9:739–748.

Gordon, S.E., J. Downing-Park, and A.L. Zimmerman. 1995. Modulation of the cGMP-gated ion channel in frog rods by calmodulin

and an endogenous inhibitory factor. *J. Physiol.* 486:533–546.

Gray-Keller, M.P., and P.B. Detwiler. 1994. The calcium feedback signal in the phototransduction cascade of vertebrate rods. *Neuron.* 13:849–861.

Grunwald, M.E., W.P. Yu, H.H. Yu, and K.W. Yau. 1998. Identification of a domain on the beta-subunit of the rod cGMP-gated cation channel that mediates inhibition by calcium-calmodulin. *J. Biol. Chem.* 273:9148–9157.

Guy, H.R., S.R. Durell, J. Warmke, R. Drysdale, and B. Ganetzky. 1991. Similarities in amino acid sequences of *Drosophila* eag and cyclic nucleotide-gated channels. *Science.* 254:730.

Hackos, D.H., and J.I. Korenbrot. 1997. Calcium modulation of ligand affinity in the cyclic GMP-gated ion channels of cone photoreceptors. *J. Gen. Physiol.* 110:515–528.

Hamill, O.P., A. Marty, E. Neher, B. Sakmann, and F.J. Sigworth. 1981. Improved patch-clamp techniques for high-resolution current recording from cells and cell-free membrane patches. *Pflugers Arch.* 391:85–100.

Heim, R., and R.Y. Tsien. 1996. Engineering green fluorescent protein for improved brightness, longer wavelengths and fluorescence resonance energy transfer. *Curr. Biol.* 6:178–182.

Hsu, Y.T., and R.S. Molday. 1993. Modulation of the cGMP-gated channel of rod photoreceptor cells by calmodulin. *Nature.* 361: 76–79.

Hsu, Y.T., and R.S. Molday. 1994. Interaction of calmodulin with the cyclic GMP-gated channel of rod photoreceptor cells. Modulation of activity, affinity purification, and localization. *J. Biol. Chem.* 269:29765–29770.

Jan, L.Y., and Y.N. Jan. 1990. A superfamily of ion channels. *Nature.* 345:672.

Jiang, Y., A. Lee, J. Chen, M. Cadene, B.T. Chait, and R. MacKinnon. 2002. The open pore conformation of potassium channels. *Nature.* 417:523–526.

Kaupp, U.B., and R. Seifert. 2002. Cyclic nucleotide-gated ion channels. *Physiol. Rev.* 82:769–824.

Kaupp, U.B., T. Niidome, T. Tanabe, S. Terada, W. Bonigk, W. Stuhmer, N.J. Cook, K. Kangawa, H. Matsuo, T. Hirose, et al. 1989. Primary structure and functional expression from complementary DNA of the rod photoreceptor cyclic GMP-gated channel. *Nature.* 342:762–766.

Korschen, H.G., M. Illing, R. Seifert, F. Sesti, A. Williams, S. Gotzes, C. Colville, F. Muller, A. Dose, M. Godde, et al. 1995. A 240 kDa protein represents the complete beta subunit of the cyclic nucleotide-gated channel from rod photoreceptor. *Neuron.* 15:627–636.

Koutalos, Y., K. Nakatani, and K.W. Yau. 1995. The cGMP-phosphodiesterase and its contribution to sensitivity regulation in retinal rods. *J. Gen. Physiol.* 106:891–921.

Kurahashi, T., and A. Menini. 1997. Mechanism of odorant adaptation in the olfactory receptor cell. *Nature.* 385:725–729.

Lakowicz, J.R. 1999. Principles of Fluorescence Spectroscopy. 2nd edition. Plenum Press, New York. 698 pp.

Liman, E.R., and L.B. Buck. 1994. A second subunit of the olfactory cyclic nucleotide-gated channel confers high sensitivity to cAMP. *Neuron.* 13:611–621.

Liu, M., T.Y. Chen, B. Ahamed, J. Li, and K.W. Yau. 1994. Calcium-calmodulin modulation of the olfactory cyclic nucleotide-gated cation channel. *Science.* 266:1348–1354.

Matulef, K., and W.N. Zagotta. 2003. Cyclic nucleotide-gated ion channels. *Annu. Rev. Cell Dev. Biol.* 19:23–44.

Menini, A. 1999. Calcium signalling and regulation in olfactory neurons. *Curr. Opin. Neurobiol.* 9:419–426.

Miyawaki, A., J. Llopis, R. Heim, J.M. McCaffery, J.A. Adams, M. Ikura, and R.Y. Tsien. 1997. Fluorescent indicators for Ca^{2+} based on green fluorescent proteins and calmodulin. *Nature.* 388:882–887.

Molokanova, E., B. Trivedi, A. Savchenko, and R.H. Kramer. 1997. Modulation of rod photoreceptor cyclic nucleotide-gated channels by tyrosine phosphorylation. *J. Neurosci.* 17:9068–9076.

Munger, S.D., A.P. Lane, H. Zhong, T. Leinders-Zufall, K.W. Yau, F. Zufall, and R.R. Reed. 2001. Central role of the CNGA4 channel subunit in Ca^{2+}-calmodulin-dependent odor adaptation. *Science.* 294:2172–2175.

Nakamura, T., and G.H. Gold. 1987. A cyclic nucleotide-gated conductance in olfactory receptor cilia. *Nature.* 325:442–444.

Nakatani, K., Y. Koutalos, and K.W. Yau. 1995. Ca^{2+} modulation of the cGMP-gated channel of bullfrog retinal rod photoreceptors. *J. Physiol.* 484(Pt 1):69–76.

Peng, C., E.D. Rich, C.A. Thor, and M.D. Varnum. 2003. Functionally important calmodulin-binding sites in both NH2- and COOH-terminal regions of the cone photoreceptor cyclic nucleotide-gated channel CNGB3 subunit. *J. Biol. Chem.* 278:24617–24623.

Rebrik, T.I., and J.I. Korenbrot. 1998. In intact cone photoreceptors, a Ca^{2+}-dependent, diffusible factor modulates the cGMP-gated ion channels differently than in rods. *J. Gen. Physiol.* 112: 537–548.

Richards, M.J., and S.E. Gordon. 2000. Cooperativity and cooperation in cyclic nucleotide-gated ion channels. *Biochemistry.* 39: 14003–14011.

Robinson, R.B., and S.A. Siegelbaum. 2003. Hyperpolarization-activated cation currents: from molecules to physiological function. *Annu. Rev. Physiol.* 65:453–480.

Sagoo, M.S., and L. Lagnado. 1996. The action of cytoplasmic calcium on the cGMP-activated channel in salamander rod photoreceptors. *J. Physiol.* 497(Pt 2):309–319.

Sautter, A., X. Zong, F. Hofmann, and M. Biel. 1998. An isoform of the rod photoreceptor cyclic nucleotide-gated channel beta subunit expressed in olfactory neurons. *Proc. Natl. Acad. Sci. USA.* 95: 4696–4701.

Selvin, P.R. 1995. Fluorescence resonance energy transfer. *Methods Enzymol.* 246:300–334.

Trudeau, M.C., and W.N. Zagotta. 2002a. An intersubunit interaction regultates trafficking in rod cyclic nucleotide-gated channels and is disrupted in an inherited form of blindness. *Neuron.* 34: 197–207.

Trudeau, M.C., and W.N. Zagotta. 2002b. Mechanism of calcium/calmodulin inhibition of rod cyclic nucleotide-gated channels. *Proc. Natl. Acad. Sci. USA.* 99:8424–8429.

Trudeau, M.C., and W.N. Zagotta. 2003. Calcium/calmodulin modulation of olfactory and rod cyclic nucleotide-gated ion channels. *J. Biol. Chem.* 278:18705–18708.

Varnum, M.D., and W.N. Zagotta. 1997. Interdomain interactions underlying activation of cyclic nucleotide-gated channels. *Science.* 278:110–113.

Weitz, D., M. Zoche, F. Muller, M. Beyermann, H.G. Korschen, U.B. Kaupp, and K.W. Koch. 1998. Calmodulin controls the rod photoreceptor CNG channel through an unconventional binding site in the N-terminus of the beta-subunit. *EMBO J.* 17:2273–2284.

Weitz, D., N. Ficek, E. Kremmer, P.J. Bauer, and U.B. Kaupp. 2002. Subunit stoichiometry of the CNG channel of rod photoreceptors. *Neuron.* 36:881–889.

Weyand, I., M. Godde, S. Frings, J. Weiner, F. Muller, W. Altenhofen, H. Hatt, and U.B. Kaupp. 1994. Cloning and functional expression of a cyclic-nucleotide-gated channel from mammalian sperm. *Nature.* 368:859–863.

Yau, K.W., and D.A. Baylor. 1989. Cyclic GMP-activated conductance of retinal photoreceptor cells. *Annu. Rev. Neurosci.* 12:289–327.

Zagotta, W.N., N.B. Olivier, K.D. Black, E.C. Young, R. Olson, and E. Gouaux. 2003. Structural basis for modulation and agonist specificity of HCN pacemaker channels. *Nature.* 425:200–205.

Zheng, J., and W.N. Zagotta. 2000. Gating rearrangements in cyclic nucleotide-gated channels revealed by patch-clamp fluorometry. *Neuron.* 28:369–374.

Zheng, J., and W.N. Zagotta. 2003. Patch-clamp fluorometry recording of conformational rearrangements of ion channels. *Sci STKE.* 2003:PL7.

Zheng, J., and W.N. Zagotta. 2004. Stoichiometry and assembly of olfactory cyclic nucleotide-gated channels. *Neuron.* 42:411–421.

Zheng, J., M.C. Trudeau, and W.N. Zagotta. 2002. Rod cyclic nucleotide-gated channels have a stoichiometry of three CNGA1 subunits and one CNGB1 subunit. *Neuron.* 36:891–896.

Zheng, J., M.D. Varnum, and W.N. Zagotta. 2003. Disruption of an intersubunit interaction underlies Ca^{2+}-calmodulin modulation of cyclic nucleotide-gated channels. *J. Neurosci.* 23:8167–8175.

Zhong, H., L.L. Molday, R.S. Molday, and K.W. Yau. 2002. The heteromeric cyclic nucleotide-gated channel adopts a 3A:1B stoichiometry. *Nature.* 420:193–198.

Zhou, Y., J.H. Morais-Cabral, A. Kaufman, and R. MacKinnon. 2001. Chemistry of ion coordination and hydration revealed by a K^+ channel-Fab complex at 2.0 A resolution. *Nature.* 414:43–48.

Zimmerman, A.L. 2002. Two B or not two B? Questioning the rotational symmetry of tetrameric ion channels. *Neuron.* 36:997–999.

Zufall, F., and S.D. Munger. 2001. From odor and pheromone transduction to the organization of the sense of smell. *Trends Neurosci.* 24:191–193.